Electronic Supplementary Material (ESI) for New Journal of Chemistry.

Promoting Hydrogen Evolution of g-C_3N_4 Based Photocatalyst by Indium and Phosphorus Co-doping

Xiaohang Yang,[a] Chi Cao,[a] Zilong Guo,[b] Xiaoyu Zhang,[a] Yaxin Wang[b] and Wensheng Yang*,[a,b]

[a] *State Key Laboratory of Inorganic Synthesis and Preparative Chemistry, College of Chemistry, Jilin University, Changchun 130012, China*

[b] *Institute of Molecular Plus, Tianjin University, Tianjin 300072, China*

E-mail: wsyang@jlu.edu.cn

Contents

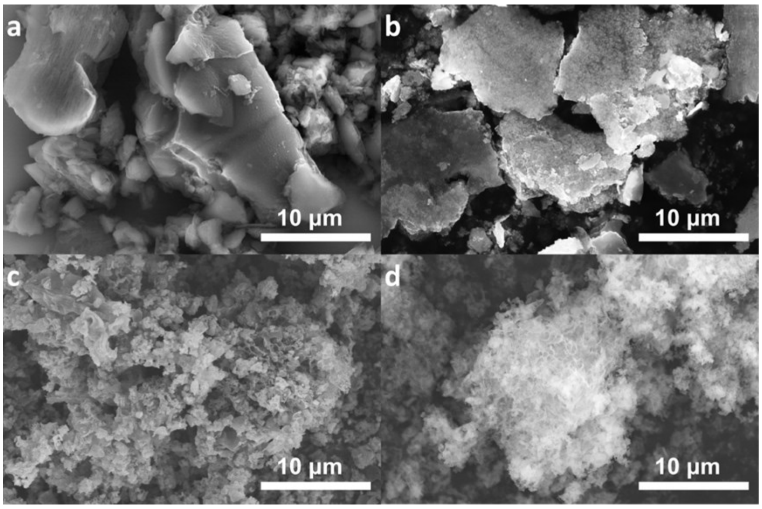

Fig. S1 SEM images of (a) g-C_3N_4, (b) In-g-C_3N_4, (c) P-g-C_3N_4 and (d) In,P-g-C_3N_4 photocatalysts. The g-C_3N_4 and In-g-C_3N_4 photocatalysts showed the similar sheet-like structure, which was absent in the images of the P-g-C_3N_4 and In,P-g-C_3N_4 photocatalysts, meaning the doping of indium have little effect on the layered structure and the doping of phosphorus destroy the layered structure to some extent.

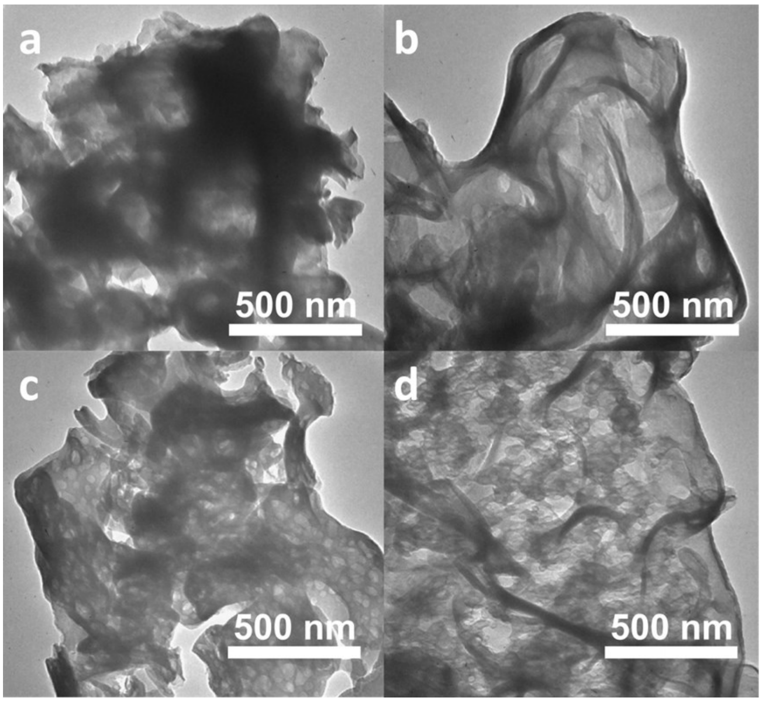

Fig. S2 TEM images of (a) g-C_3N_4, (b) In-g-C_3N_4, (c) P-g-C_3N_4 and (c) In,P-g-C_3N_4 photocatalysts. The typical two-dimensional sheet-like structure of g-C_3N_4 was observable for all the photocatalysts, meaning remaining of the layered structure upon the indium and/or phosphorus doping, consistent with the XRD results (see Fig. 2 in the text).

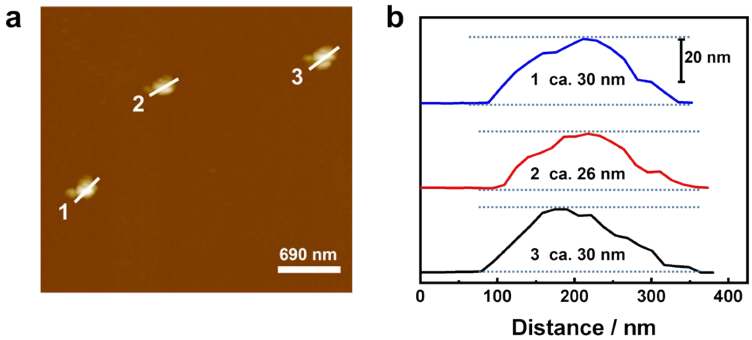

Fig. S3 (a) Tapping-mode AFM image of the In,P-g-C_3N_4 photocatalyst deposited on silicon wafer substrate and (b) Variation in height of the photocatalyst along the labeled lines. Lateral dimension of the photocatalyst was measured to be ca. 280 nm and its thickness was determined to be ca. 28 nm.

Table S1 Contents of C and N elements and the corresponding molar ratio of C and N in the g-C_3N_4, P-g-C_3N_4, In-g-C_3N_4 and In,P-g-C_3N_4 photocatalysts.

Photocatalyst	C (wt.%)	N (wt.%)	C/N (mol/mol)
g-C_3N_4	33.83	54.96	0.7181
P-g-C_3N_4	22.87	41.31	0.6458
In-g-C_3N_4	32.23	52.79	0.7123
In,P-g-C_3N_4	28.46	51.67	0.6426

Table S2 Comparison in quantum efficiency (QE) of different $g\text{-}C_3N_4$-based photocatalysts and the standard photocatalysts (Degussa P25 and CdS) at the monochromatic irradiation wavelength of 420 nm.

Catalyst	Doped element	Quantum efficiency (%)	Ref.
In-$g\text{-}C_3N_4$	In^{3+}	6.79	Ref. 18 in the text
Zn-$g\text{-}C_3N_4$	Zn^{2+}	3.20	Ref. 34 in the text
I-$g\text{-}C_3N_4$	I	2.40	Ref. 35 in the text
P-$g\text{-}C_3N_4$	P	3.56	Ref. 36 in the text
Na,P-$g\text{-}C_3N_4$	Na^{+},P	6.80	Ref. 17 in the text
In,P-$g\text{-}C_3N_4$	**In,P**	**8.02**	**This work**
P25	--	--	Ref. 32 in the text
CdS	--	0.38	Ref. 33 in the text

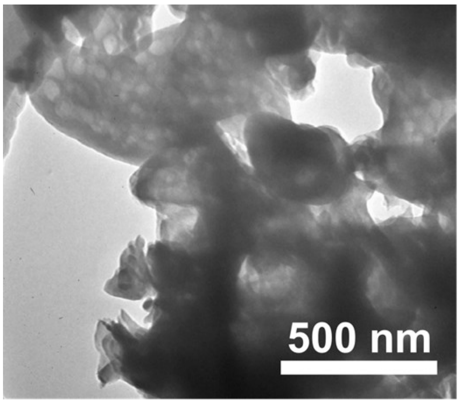

Fig. S4 TEM image of the In,P-g-C_3N_4 photocatalyst after four cycles of the H_2 generation reaction. No obvious changes in morphology of the In,P-g-C_3N_4 photocatalyst could be observed after the reaction (see Fig. S2 for comparison).

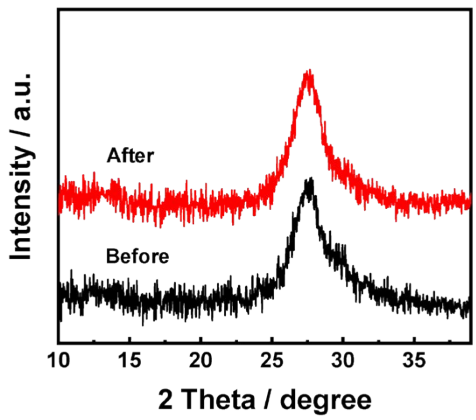

Fig. S5 Comparison in XRD patterns of the In,P-g-C_3N_4 photocatalyst before (black) and after (red) four cycles of the H_2 generation reaction. There were almost no differences in position and intensity of XRD peaks for the photocatalyst before and after the reaction.

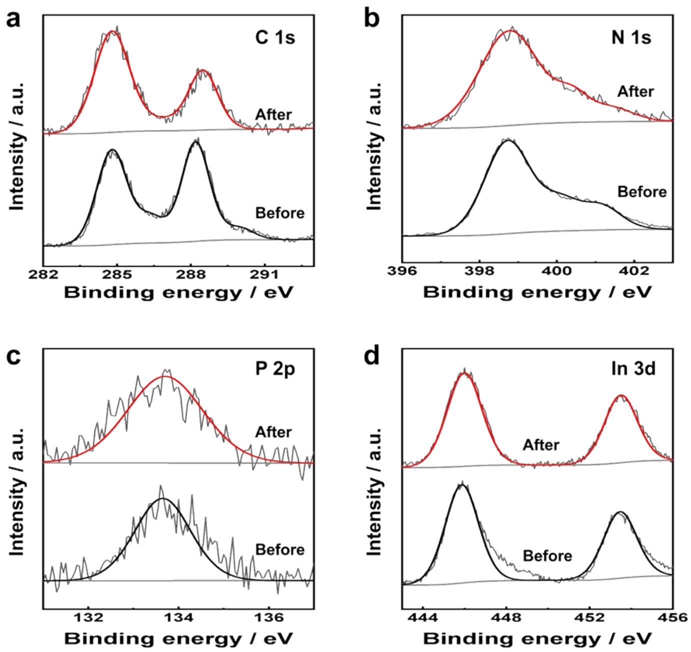

Fig. S6 Comparison in high resolution (a) C 1s, (b) N 1s, (c) P 2p, and (d) In 3d XPS spectra of the In,P-g-C_3N_4 photocatalyst before (black) and after (red) four cycles of the H_2 generation reaction. There were almost no changes in XPS spectra of the photocatalyst before and after the reaction.

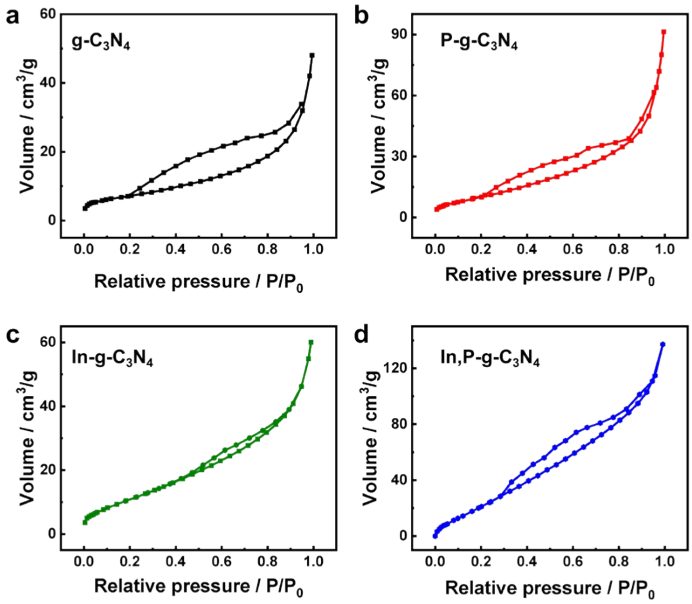

Fig. S7 Nitrogen adsorption-desorption isotherms of the (a) g-C_3N_4, (b) P-g-C_3N_4, (c) In-g-C_3N_4 and (d) In,P-g-C_3N_4 photocatalysts (see Table S3 for the derived surface areas and pore volumes).

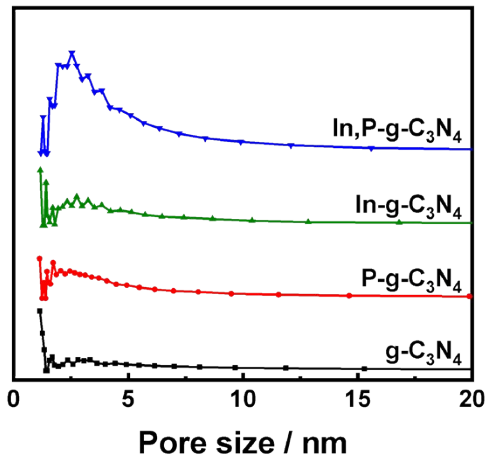

Fig. S8 Size distribution curves of the g-C_3N_4, P-g-C_3N_4, In-g-C_3N_4 and In,P-g-C_3N_4 photocatalysts (see Table S3 for the derived average pore sizes).

Table S3 Surface areas, pore volumes and average pore sizes of the g-C_3N_4, P-g-C_3N_4, In-g-C_3N_4 and In,P-g-C_3N_4 photocatalysts.

Sample	Surface area ($m^2 \cdot g^{-1}$)	Pore volume ($cm^3 \cdot g^{-1}$)	Average pore size (nm)
g-C_3N_4	24.91	0.07	1.65
P-g-C_3N_4	37.05	0.14	2.46
In-g-C_3N_4	34.81	0.09	2.27
In,P-g-C_3N_4	73.57	0.21	2.77

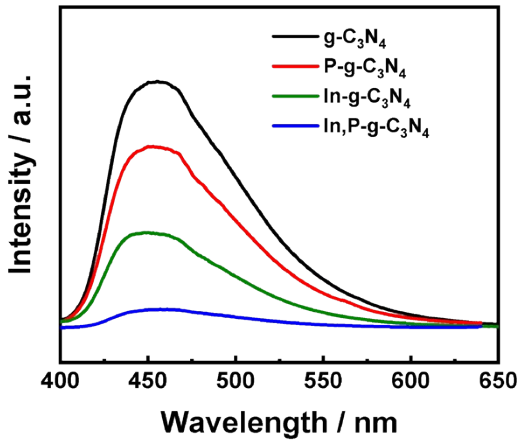

Fig. S9 Photoluminescence spectra of the g-C_3N_4, P-g-C_3N_4, In-g-C_3N_4 and In,P-g-C_3N_4 photocatalysts. Intensity of the emission peak of g-C_3N_4 at 452 nm decreased upon the doping of indium or phosphorus, indicating the indium or phosphorus doping is effective to suppress the recombination of photogenerated electron-hole pairs. The emission was weakened greatly in the In,P-g-C_3N_4, implying the synergistic effect of In and P doping on improving the separation efficiency of photogenerated charge carriers.

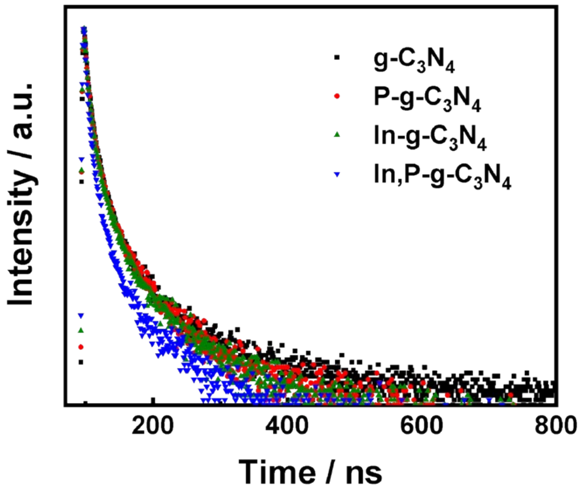

Fig. S10 Time-resolved photoluminescence decay spectra of the g-C_3N_4, P-g-C_3N_4, In-g-C_3N_4 and In,P-g-C_3N_4 photocatalysts. The triexponential decay function was utilized to fit the curves (see Table S4 for the fitting results).

Table S4. Room temperature transient fluorescence decay of g-C_3N_4, P-g-C_3N_4, In-g-C_3N_4 and In,P-g-C_3N_4 catalysts.

Samples	Parameters	Lifetime (ns)	Relative percentage (%)	Average lifetime (ns)
g-C_3N_4	τ_1	9.11	38.25	3.34
	τ_2	63.48	10.92	
	τ_3	1.98	50.83	
P-g-C_3N_4	τ_1	9.08	38.01	3.14
	τ_2	62.02	11.98	
	τ_3	1.82	50.00	
In-g-C_3N_4	τ_1	8.11	38.90	2.90
	τ_2	57.02	12.16	
	τ_3	1.66	48.94	
In,P-g-C_3N_4	τ_1	6.05	33.27	1.95
	τ_2	49.27	10.30	
	τ_3	1.24	56.43	

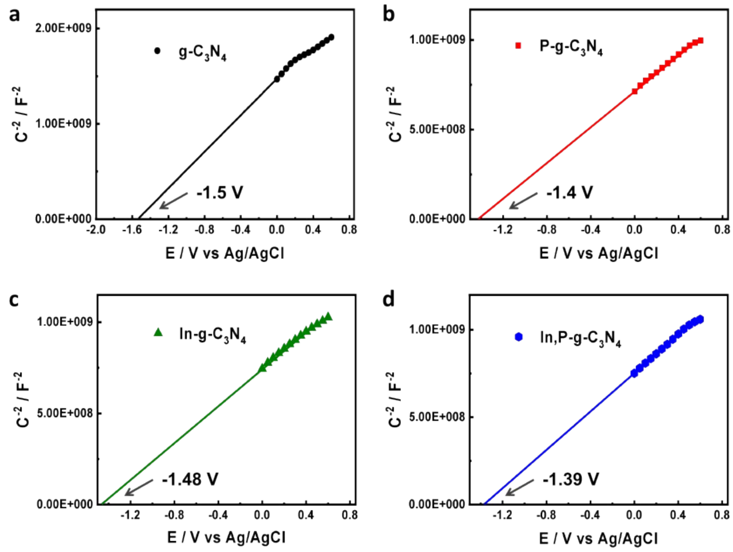

Fig. S11 Mott-Schottky plots of the (a) g-C_3N_4, (b) P-g-C_3N_4, (c) In-g-C_3N_4 and (d) In,P-g-C_3N_4 photocatalysts. According to the X intercepts at the tangents of plots, flat band potentials (E_{fb}) of the g-C_3N_4, P-g-C_3N_4, In-g-C_3N_4 and In,P-g-C_3N_4 photocatalysts were derived to be -1.50, -1.40, -1.48 and -1.39 V (vs. Ag/AgCl), and -0.91, -0.81, -0.89 and -0.80 V (vs. NHE, pH=0), respectively (see Ref. 32 in the text). By assuming the conduction band minimum (CBM) of the n-type semiconductor be 0.1 V more negative than the E_{fb} values (see Ref. 32 in the text), the corresponding CBM potentials of the g-C_3N_4, P-g-C_3N_4, In-g-C_3N_4 and In,P-g-C_3N_4 photocatalysts were thus derived to be -1.01, -0.91, -0.99 and -0.90 V (vs. NHE, pH=0), respectively.

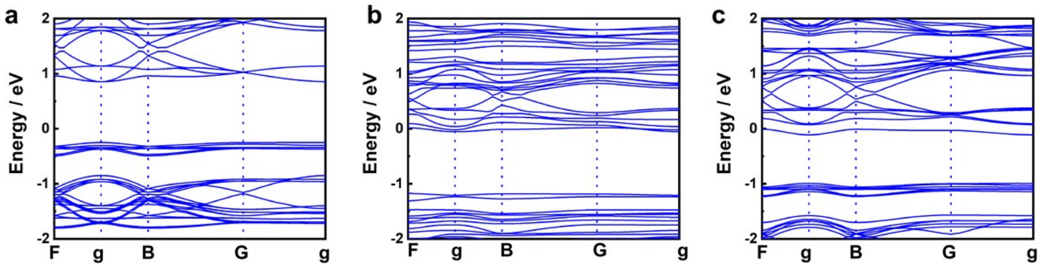

Fig. S12 The calculated band structures of the (a) g-C_3N_4, (b) In-g-C_3N_4 and (c) P-g-C_3N_4 photocatalysts. The corresponding total density of states (TDOS) and projected density of states (pDOS) contributed by orbitals of the constituent atoms were shown in Fig.7 in the text.